Samantha Hall is currently pursuing a B.S. in biomedical engineering with a minor in biology and is expected to graduate in May of 2023. Additionally, she is pursing graduate level coursework through the biomedical engineering Accelerated B.S. to M.S. program. She has worked in Dr. Joel D. Bumgardner's lab since January of 2021 and is primarily involved in studies regarding macrophage polarization. Samantha is involved in the Society of Women Engineers, Tau Beta Pi Honor Society, and Tennessee Louis Stokes Alliance for Minority Participation. In the future, she plans on pursuing a PhD in biomedical engineering as well as a career in biomaterials research.

Samantha Hall, Malika Rad

& Joel D. Bumgardner

Analysis of In-vivo Macrophage Polarization in Response to Raspberry Ketone-Loaded Chitosan Membranes for Guided Bone Regeneration

Faculty Sponsor

Dr. Joel D. Bumgardner

Abstract

Nanofibrous electrospun chitosan membranes (ESCMs) have shown promise for enhanced guided bone regeneration (GBR) in alveolar defects when insufficient bone volume is present. Following GBR, a strategy that can be implemented to facilitate healing is the promotion of macrophage polarization from a pro-inflammatory phenotype (M1) to an anti-inflammatory phenotype (M2). Raspberry ketone (RK) is a natural compound that possesses anti-inflammatory properties. ESCMs were used to locally deliver RK to an in-vivo bone defect site using a rat calvarial model. ESCMs were loaded with 0 or 250 μg RK. Membranes from each treatment were implanted into rat calvarial defects (n=8). Membranes and surrounding tissues were extracted in serial sections and immunohistochemically stained at 1, 2, and 4 weeks using individual markers for M1(iNOS), M2 (CD206), and total macrophages (CD68). Percent-stained area was quantified using NIH ImageJ. Results indicated that ESCMs loaded with 250 μg RK facilitated M1 to M2 macrophage polarization.

Introduction

Alveolar bone loss can occur in patients due to periodontal disease or trauma. In the U.S. alone, more than 50% of adults suffer from periodontal disease (Eke 2012). This condition can become more prevalent as patient age increases. Furthermore, alveolar bone loss directly affects both patient health and patient quality of life. To combat these issues, a procedure called guided bone regeneration is often employed. Due to insufficient bone volume being present, Guided Bone Regeneration (GBR) is a surgical procedure that replaces missing bone with material from a patient's own body or with an artificial, synthetic, or natural substitute (Kumar 2013). As shown in Figure 1, when employing the procedure, a supporting material is placed into the socket where the bone is missing (Rodriguez 2018).

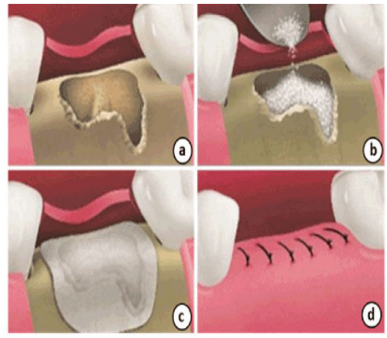

Figure 1. Guided Bone Regeneration procedure used to combat bone loss. (Rodriguez 2018)

A barrier membrane is then used to create a partition between the new bone growth and the soft tissues. However, complications can arise when connective and epithelial tissues invade the defect site, resulting in inadequate bone tissue regeneration. For healing to occur after the barrier membrane has been implanted, the inflammatory phase of the wound healing process must transition to the proliferative phase.

A type of cell that plays a prominent role in all phases of the wound healing process is the macrophage. Macrophages are specialized cells that originate from a type of immune cell called monocytes. Monocytes are attracted to tissues in response to injury, and these cells differentiate into macrophages. Macrophages are involved in the detection, phagocytosis, and destruction of bacteria (Rodriguez 2018). In relation to environmental signals, macrophages can differentiate into distinct populations. Specifically,

macrophages undergo a polarization along a spectrum into their M1 and M2 phenotypes. M1 macrophages are pro-inflammatory and possess antimicrobial properties while M2 macrophages are anti-inflammatory and aid in immune regulation (Fujiwara & Kobayashi 2005). As shown in Figure 2, M1 macrophages are introduced during the inflammatory phase of wound healing, and they polarize to their pro-healing M2 phenotype as tissue formation occurs in the proliferative phase. Moreover, M1 macrophages initiate the tissue repair process while M2 macrophages stabilize the repair process. Therefore, as the wound healing process progresses, M1 macrophages begin to polarize from their M1 phenotype to their M2 phenotype.

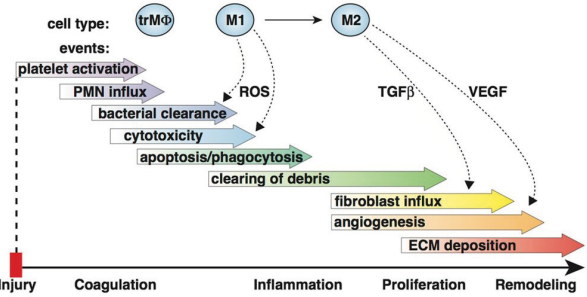

Figure 2. Diagram of macrophage polarization throughout the wound healing process. (Boniakowski et al., 2017)

This polarization was evaluated during an in-vitro study conducted in our lab that examined macrophage polarization from the M1 phenotype to the M2 phenotype in response to different concentrations of raspberry ketone (RK). RK is a natural phenolic compound of red raspberry that is known for its antioxidant and anti-inflammatory properties (Krzyszczyk 2018). Due to its anti-inflammatory properties, RK has shown potential in facilitating macrophage polarization. The in-vitro study found that raspberry ketone increased anti-inflammatory cytokines and decreased proinflammatory cytokines, which are signaling molecules that are specific to macrophage phenotypes and initiate healing properties.

To promote soft tissue healing and bone regeneration in the GBR process through the stimulation of macrophage polarization, the current study uses electrospun chitosan membranes (ESCMs) to locally deliver RK to an in-vivo bone defect site using a rat calvarial model. This will then allow the following questions to be answered:

1- Does RK affect macrophage polarization?

2- Does RK increase the number of anti-inflammatory, M2, macrophages?

Materials and Methods

Nanofibrous electrospun membranes composed of the natural polymer, chitosan, were loaded with RK. Chitosan is a polymer that is synthesized from chitin, a polysaccharide widely distributed in nature (Dodane et al.,1998). Moreover, Chitosan is appropriate for use as a membrane material in guided bone regeneration due to its resorbable nature, biocompatibility, and controlled degradation properties. Additionally, the nanofibrous structure of the membranes provides an increased surface area to volume ratio, allowing for local drug delivery to stimulate healing. This study utilized chitosan membranes that were loaded with a 250 μg dose of RK. These membranes were implanted into the calvarial defects of 8 rats (n=8) for 1, 2, and 4 weeks. Bilaterally separated by the sagittal suture, each rat received one chitosan membrane that was loaded with 250 μg RK and one membrane loaded with 0 μg RK, serving as a control group as shown in Figure 3.

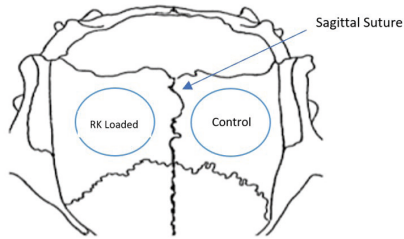

Figure 3. Rat cavlvarial defect model with RK loaded and non RK loaded chitosan membranes.

As rats were euthanized at each time point, three serial sections of tissue were extracted from each animal. The membranes and surrounding tissues were extracted in sagittal sections with a thickness of 5 microns, and an inflammatory score was given by a pathologist. As shown in Figure 4, these sections were immunohistochemically stained with CD68, CD206, and iNOS. These markers stained for the presence of all macrophages, M2 macrophages, or M1 macrophages, respectively. As shown in Figure 5, images of these immunohistochemically stained tissues were taken at 20X magnification using the image stitching function of an Olympus microscope. Images were analyzed by a blind observer using NIH ImageJ.

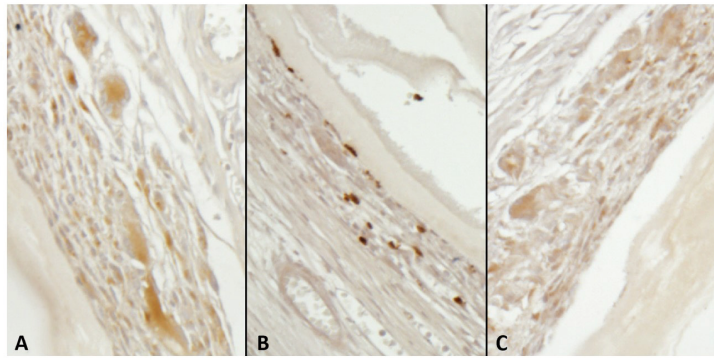

Figure 4. Immunohistochemical staining using CD68 (A), CD206 (B), and iNOS (C) for total, M1, and M2 macrophages, respectively.

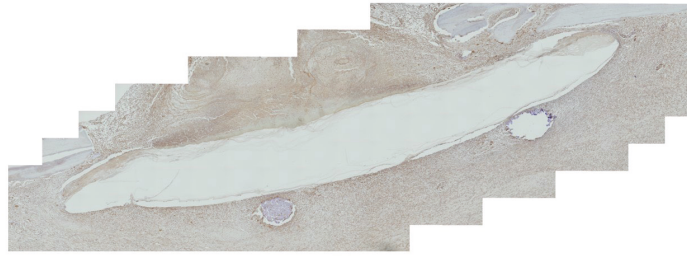

Figure 5. Immunohistochemically stained sample including membrane and surrounding tissue.

Using NIH ImageJ, the macrophages present in the inflammatory area of the membrane's surrounding tissue were quantified autonomously. Specifically, the inflammatory and the membrane areas were identified and isolated. Then, each tissue image was separated into three color channels using color deconvolution. As shown in Figure 6, using the orange color channel, the threshold intensity was manually adjusted to adequately cover the macrophage staining area, which was shown in brown. The size of cell (100-infinity pixel2) and the circularity (0-2) were constant values for all tissue sections. However, the threshold intensity was different for each tissue sample due to differences in staining intensity. The program automatically counted and outlined all macrophages based upon the set parameters, producing a binary image as shown in Figure 7.

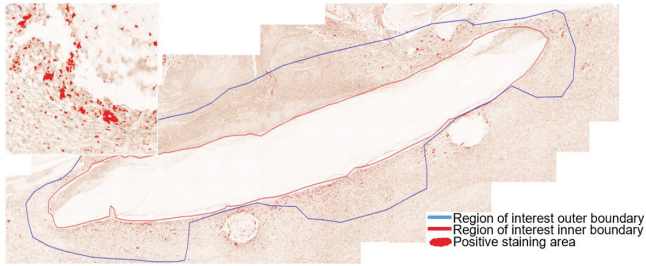

Figure 6. Membrane with isolated inflammatory region and highlighted positive macrophage staining

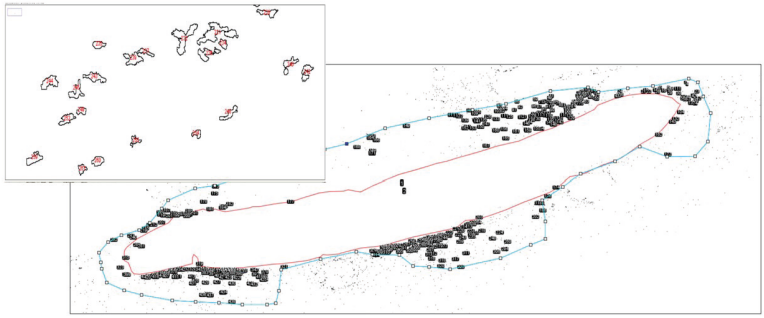

Figure 7. Binary image with individually counted macrophages.

The total area, membrane area, and stained area were also provided. All analysis utilized percent area as calculated in Equation 1.

$$\%\ Area\ (Pixel^2) = \left(\frac{Stained\ Area}{Total\ Area}\right) \times 100 \qquad (1)$$

Percent area was used as opposed to macrophage cell count to combat differences between animals and tissue samples as well as to compare the data to previous studies. At the completion of data compilation, a two-way ANOVA was performed for each of the three markers to identify any statistically significant differences between treatment groups and time.

Results

Figures 8, 9, and 10 display graphs of the average percent area for each treatment group at week 1, week 2, and week 3. Because staining was done on separate serial sections of tissue, total macrophage staining does not

equate the sum of M1 and M2 macrophage staining. As shown in Figure 8, the 250 µg RK treatment group had fewer total macrophages at weeks 2 and 4 and greater total macrophages at week 1. As shown in Figure 9, at the M1 macrophage week 2 timepoint, the control group had a greater number of M1 macrophages present. In Figure 10, at the M2 macrophage week 2 timepoint the 250 µg RK treatment group had a greater amount of M2 macrophages present.

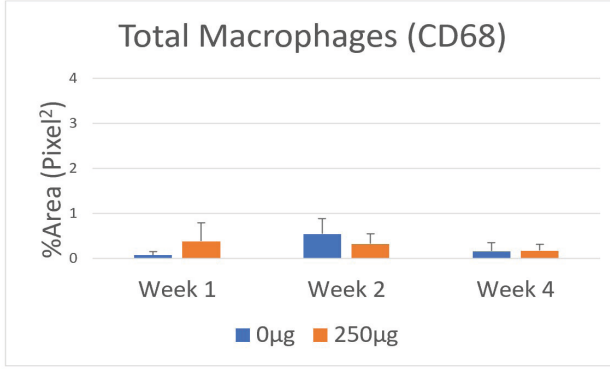

Figure 8. Total macrophage percent area data for 250 µg and 0 µg treatment group at 1, 2, and 4 weeks.

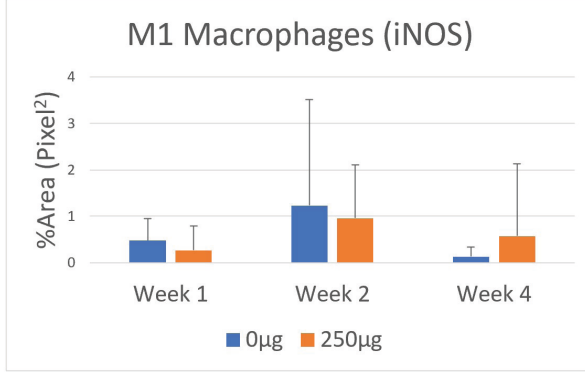

Figure 9. M1 macrophage percent area data for 250 µg and 0 µg treatment group at 1, 2, and 4 weeks.

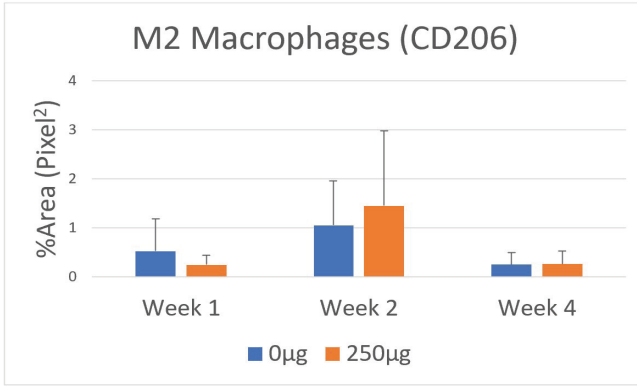

Figure 10. M2 macrophage percent area data for 250 µg and 0 µg treatment group at 1, 2, and 4 weeks.

Outliers based on the 1.5 IQR were also determined using a series of boxplots for both treatment groups for each different macrophage marker as shown in Figures 11, 12, and 13. Outliers were present for the total macrophage and M1 markers.

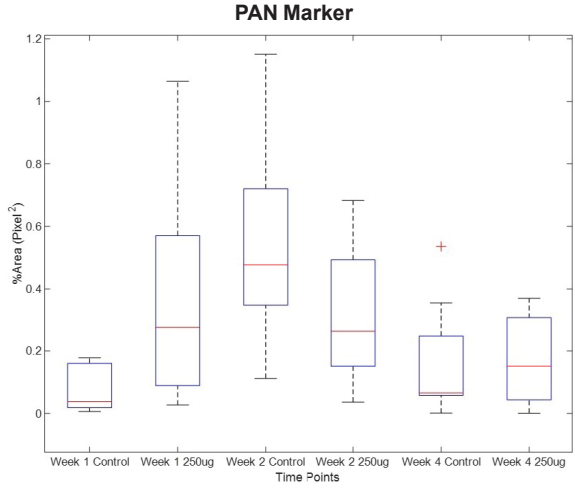

Figure 11. Boxplots of %Area for CD68 for each treatment group and time point (n=8). Red crosses indicate outliers according to upper and lower limits of Q3 + 1.5 IQR and Q1 – 1.5 IQR, respectively.

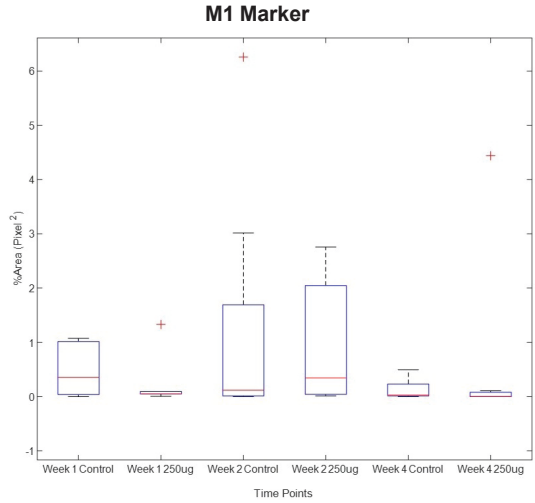

Figure 12. Boxplots of the %Area for iNOS for each treatment group and time point (n=8). Red crosses indicate outliers according to upper and lower limits of Q3 + 1.5 IQR and Q1 – 1.5 IQR, respectively.

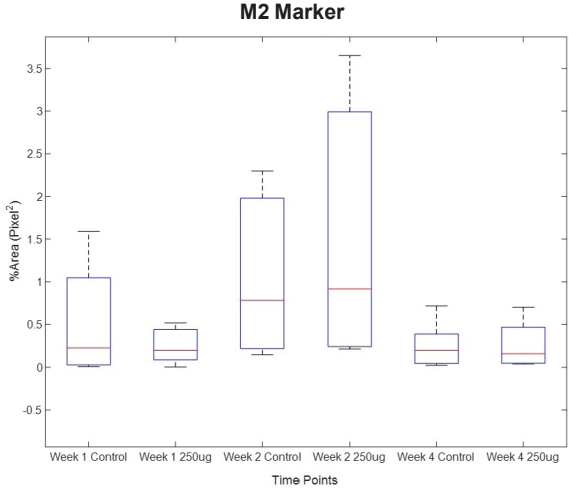

Figure 13. Boxplots of the %Area for CD206 for each treatment group and time point (n=8). Red crosses indicate outliers according to upper and lower limits of Q3 + 1.5 IQR

As shown in the Table 1 two-way ANOVA results, for all three macrophage markers, $p>0.05$ for interactions, indicating that there were no statistically significant interactions. In addition, $p>0.05$ for treatment groups for all three markers. However, $p<0.05$ for time points for CD68 and CD206, and $p>0.05$ for time points for iNOS.

Marker	Interaction	Variable	P-Value
M1 (iNOS)	0.3936	treatment	0.9966
		time	0.0003
M2 (CD206)	0.4157	treatment	0.6634
		time	0.2763
PAN (CD68)	0.1437	treatment	0.9714
		time	0.0062

Table 1. Results of two-way ANOVA

Discussion

The results of the two-way ANOVA show that there was no statistically significant difference between the control group and the 250 μg RK treatment group. However, apart from the M1 marker, which could potentially be due to the presence of outliers, there was a statistically significant difference between time points. The statistical difference between time points is an indicator of macrophage polarization taking place for both treatment groups. This indicates that the wound healing process was able to naturally occur, and the raspberry ketone did not inhibit macrophage polarization.

Although no statistical differences between groups were noted, trends were present throughout the data, indicating that RK did influence macrophage polarization. For total macrophages, on average, the 250 μg RK treatment group had fewer overall macrophages at weeks 2 and 4 and greater overall macrophages at week 1. Early in the wound healing process, macrophage cell counts would be expected to increase as M1 macrophages are introduced, clearing out debris and pathogens. The cell count would then decrease after macrophages transition to their pro-healing M2 phenotype. Macrophages are no longer required as wound healing progresses and tissue formation occurs. Therefore, this total macrophage trend is indicative of the 250 μg RK treatment group being further ahead in the polarization process in comparison to the control group. The M1 macrophage week 2 timepoint shows that the control group had a greater amount of M1 macrophages present, and the M2 macrophage week 2 timepoint shows that the 250 μg RK treatment group had a greater amount of M2 macrophages present. This trend also indicates that the 250 μg RK treatment group had a quicker M1 to M2 polarization in comparison to the control group.

The increased polarization toward the M2 phenotype that these trends exhibit is indicative of the progression of the wound healing process. As previously stated, M2 macrophages are pro-healing. Therefore, increased polarization toward the M2 phenotype indicates increased bone regeneration.

Conclusion

Graphically, it appears that raspberry ketone influences the polarization of macrophages from the M1 to the M2 phenotype in rat calvarial defects. Specifically, the graphed data indicates a lower amount of M1 macrophages and a higher amount of M2 macrophages in the RK treated group, indicating increased polarization and bone regeneration. For future studies, larger sample sizes could be used to increase the statistical significance and to further validate findings. Additionally, due to the presence of large standard deviations, the accuracy of individual markers could be explored. Furthermore, other doses of RK should be analyzed for dose dependent effects.

References

[1] Eke, Paul I., B. A. Dye, Li Wei, G. O. Thornton-Evans, and R. J. Genco. "Prevalence of periodontitis in adults in the United States: 2009 and 2010." Journal of dental research 91, no. 10 (2012): 914-920.

[2] Kumar, Prasanna, Belliappa Vinitha, and Ghousia Fathima. "Bone grafts in dentistry." Journal of pharmacy & bioallied sciences 5, no. Suppl 1 (2013): S125.

[3] Rodriguez, I. A., G. S. Selders, A. E. Fetz, C. J. Gehrmann, S. H. Stein, J. A. Evensky, M. S. Green, and G. L. Bowlin. "Barrier membranes for dental applications: A review and sweet advancement in membrane developments." Mouth Teeth 2, no. 1 (2018): 1-9.

[4] Krzyszczyk, Paulina, Rene Schloss, Andre Palmer, and François Berthiaume. "The role of macrophages in acute and chronic wound healing and interventions to promote pro-wound healing phenotypes." Frontiers in physiology 9 (2018): 419.

[5] Fujiwara, Nagatoshi, and Kazuo Kobayashi. "Macrophages in inflammation." Current Drug Targets-Inflammation & Allergy 4, no. 3 (2005): 281-286.

[6] Boniakowski, Anna E., Andrew S. Kimball, Benjamin N. Jacobs, Steven L. Kunkel, and Katherine A. Gallagher. "Macrophage-mediated inflammation in normal and diabetic wound healing." The Journal of Immunology 199, no. 1 (2017): 17-24.

[7] Dodane, Valérie, and Vinod D. Vilivalam. "Pharmaceutical applications of chitosan." Pharmaceutical Science & Technology Today 1, no. 6 (1998): 246-253.